Quantitative CT of the knee in the IMI-APPROACH osteoarthritis cohort: association of bone mineral density with radiographic disease severity, meniscal coverage and meniscal extrusion

Heiss, R.; Laredo, J.D.; Wirth, W.; Jansen, M.P.; Marijnissen, A.C.A.; Lafeber, F.; ... ; Roemer, F.W.

Bone 168 (2023) 116673

Contents lists available at ScienceDirect

Bone

journal homepage: www.elsevier.com/locate/bone

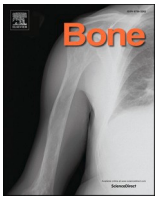

Full Length Article

Quantitative CT of the knee in the IMI-APPROACH osteoarthritis cohort: Association of bone mineral density with radiographic disease severity, meniscal coverage and meniscal extrusion

Rafael Heiss [a,*], Jean-Denis Laredo [b,c], Wolfgang Wirth [d,e,f], Mylène P. Jansen [g], Anne C. A. Marijnissen [g], Floris Lafeber [g], Agnes Lalande [h], Harrie H. Weinans [i], Francisco J. Blanco [j,q], Francis Berenbaum [k], Margreet Kloppenburg [l], Ida K. Haugen [m], Klaus Engelke [n,o,1], Frank W. Roemer [a,p,1]

[a] Department of Radiology, Universitätsklinikum Erlangen & Friedrich-Alexander-Universität (FAU) Erlangen-Nürnberg, Maximiliansplatz 3, 91054 Erlangen, Germany
[b] Service de Radiologie, Institut Mutualiste Montsouris, 42 Bd Jourdan, 75014 Paris, France
[c] Bioimagerie Ostéo-articulaires (B3OA), UMR, CNRS, 7052 INSERM U1271,10 Avenue de Verdun, 75010 Paris, France
[d] Department of Imaging & Functional Musculoskeletal Research, Institute of Anatomy & Cell Biology, Paracelsus Medical University Salzburg & Nuremberg, Strubergasse 21, 5020 Salzburg, Austria
[e] Ludwig Boltzmann Inst. for Arthritis and Rehabilitation, Paracelsus Medical University Salzburg & Nuremberg, Strubergasse 21, 5020 Salzburg, Austria
[f] Chondrometrics GmbH, Ludwig-Zeller-Straße 12, 83395 Freilassing, Germany
[g] Department of Rheumatology & Clinical Immunology, University Medical Center Utrecht, Heidelberglaan 100, 3584, CX, Utrecht, the Netherlands.
[h] Servier, 50 rue Carnot, 92284 Suresnes cedex, France
[i] Department of Orthopaedics, University Medical Center Utrecht, Heidelberglaan 100, 3584 CX Utrecht, the Netherlands.
[j] Grupo de Investigación de Reumatología (GIR), INIBIC – Complejo Hospitalario Universitario de A Coruña, SERGAS, Centro de Investigación CICA, Departamento de Fisioterapia y Medicina, Universidad de A Coruña, A Coruña, Spain
[k] Sorbonne University, Inserm, APHP Hôpital Saint-Antoine, 75571 Paris cedex 12, France
[l] Departments of Rheumatology, Clinical Epidemiology, Leiden University Medical Center, Albinusdreef 2, 2333, ZA, Leiden, Netherlands
[m] Diakonhjemmet Hospital, Diakonveien 12, 0370 Oslo, Norway
[n] Department of Immunology and Rheumatology, Universitätsklinikum Erlangen, Friedrich-Alexander-Universität (FAU) Erlangen-Nürnberg, Ulmenweg 18, Erlangen, Germany
[o] Institute of Medical Physics, Friedrich-Alexander-Universität (FAU) Erlangen-Nürnberg, Henkestr. 91, 91052 Erlangen, Germany
[p] Boston University School of Medicine, 72 E Concord St, Boston, MA, 02118, MA, USA
[q] Servicio de Reumatologia, INIBIC- Universidade de A Coruña, As Xubias 84, 15006 A Coruña, Spain

ARTICLE INFO

Keywords:
Osteoarthritis
Knee
Quantitative CT
Bone mineral density
Multicenter study

ABSTRACT

Objective: Osteoarthritis (OA) is a highly prevalent chronic condition. The subchondral bone plays an important role in onset and progression of OA making it a potential treatment target for disease-modifying therapeutic approaches. However, little is known about changes of periarticular bone mineral density (BMD) in OA and its relation to meniscal coverage and meniscal extrusion at the knee. Thus, the aim of this study was to describe periarticular BMD in the Applied Public-Private Research enabling OsteoArthritis Clinical Headway (APPROACH) cohort at the knee and to analyze the association with structural disease severity, meniscal coverage and meniscal extrusion.

Design: Quantitative CT (QCT), MRI and radiographic examinations were acquired in 275 patients with knee osteoarthritis (OA). QCT was used to assess BMD at the femur and tibia, at the cortical bone plate (Cort) and at the epiphysis at three locations: subchondral (Sub), mid-epiphysis (Mid) and adjacent to the physis (Juxta). BMD was evaluated for the medial and lateral compartment separately and for subregions covered and not covered by the meniscus. Radiographs were used to determine the femorotibial angle and were evaluated according to the Kellgren and Lawrence (KL) system. Meniscal extrusion was assessed from 0 to 3.

Results: Mean BMD differed significantly between each anatomic location at both the femur and tibia ($p < 0.001$) in patients with KL0. Tibial regions assumed to be covered with meniscus in patients with KL0 showed lower

* Corresponding author at: Department of Radiology, Maximiliansplatz 3, 91054 Erlangen, Germany.
E-mail address: Rafael.Heiss@uk-erlangen.de (R. Heiss).
[1] Shared last authorship

https://doi.org/10.1016/j.bone.2023.116673
Received 19 October 2022; Received in revised form 16 December 2022; Accepted 4 January 2023
Available online 7 January 2023

BMD at Sub ($p < 0.001$), equivalent BMD at Mid ($p = 0.07$) and higher BMD at Juxta ($p < 0.001$) subregions compared to regions not covered with meniscus. Knees with KL2–4 showed lower Sub ($p = 0.03$), Mid ($p = 0.01$) and Juxta ($p < 0.05$) BMD at the medial femur compared to KL0/1. Meniscal extrusion grade 2 and 3 was associated with greater BMD at the tibial Cort ($p < 0.001$, $p = 0.007$). Varus malalignment is associated with significant greater BMD at the medial femur and at the medial tibia at all anatomic locations.
Conclusion: BMD within the epiphyses of the tibia and femur decreases with increasing distance from the articular surface. Knees with structural OA (KL2–4) exhibit greater cortical BMD values at the tibia and lower BMD at the femur at the subchondral level and levels beneath compared to KL0/1. BMD at the tibial cortical bone plate is greater in patients with meniscal extrusion grade 2/3.

1. Introduction

Osteoarthritis (OA) of the knee joint has a high prevalence with marked implications for patients and public health care [1,2]. Symptomatic knee OA affects almost 10 % of the United States population by age 60 [3]. During the course of the disease the subchondral bone plate becomes sclerotic and formation of osteophytes and subchondral cysts is observed [4]. Thickening and disruption of the normal periarticular trabecular architecture occurs early in the disease, and may precede cartilage damage [5–7]. During the course of the disease the subchondral epiphyseal trabecular network undergoes remodeling as a result of altered biomechanical loading [8]. The subchondral bone plays an important role in onset and progression of disease making it a potential treatment target for disease-modifying therapeutic approaches [7,9,10].

Quantitative computed tomography (QCT) is an established method for the non-invasive assessment of local bone mineral density (BMD) for both ex-vivo and in-vivo analyses and enables a quantitative, reproducible depiction of periarticular bone changes [7,11–13]. Interestingly, in-vivo changes of periarticular BMD of the femur and tibia in OA have rarely been investigated and the relationship of structural disease severity or meniscal coverage and extrusion with BMD changes in different anatomic levels and locations within the epiphysis have not been reported to date [14,15]. The quantification of subchondral BMD at the tibial and femoral epiphysis may be an important piece in the puzzle of our pathophysiological understanding of OA and has potential as a biomarker to monitor disease progression [7,16].

As part of the exploratory, European, 5-centre, 2-year prospective follow-up cohort project Innovative Medicines Initiative - Applied Public-Private Research enabling OsteoArthritis Clinical Headway (IMI-APPROACH) conventional and novel clinical, imaging, and biochemical biomarkers were applied to prospectively describe pre-identified progressor phenotypes of patients with symptomatic and/or structural knee OA including QCT, X-ray, and semiquantitative MRI scoring of features of OA [17].

We hypothesized that cortical and subchondral BMD differs between different anatomic locations of the tibial and femoral epiphysis in structurally normal knees. In addition, we hypothesized that subchondral BMD at the tibia may be affected by meniscal coverage and that BMD will be higher with increasing structural disease severity and with the extent of meniscal extrusion, likely in conjunction with increasing sclerotic changes and remodeling.

Thus, the purpose of this study was 1) to describe in symptomatic patients without radiographic knee OA (KL0) epiphyseal BMD at distinct anatomic locations of the femur and tibia in regard to the distance of the articular surface and regarding the comparison between the medial and lateral compartment. Additional aims of the study were 2) to assess the influence of assumed meniscal coverage at the tibia on BMD values in KL0 knees, 3) to evaluate the association of BMD at different locations with structural OA disease severity and 4) with the extent of meniscal extrusion.

2. Methods

2.1. Study sample

297 patients with clinical and/or structural knee OA were included in the IMI-APPROACH cohort study enrolled at five clinical centers in Europe [17,18]. Study recruitment was based on five existing observational OA cohorts (CHECK (Utrecht, The Netherlands) [19], HOSTAS (Leiden, The Netherlands) [20], MUST (Oslo, Norway) [21], PROCOAC (A Coruña, Spain) [22], and DIGICOD (Paris, France) [23] or from outpatient departments, if not enough participants could be recruited from these existing cohorts. The recruitment for IMI-APPROACH was based on historical data used to train machine learning models to estimate the likelihood of joint space width loss and/or increased or sustained knee pain over the course of the study from demographic data, pain scores, and radiographic features [24]. An index knee was defined at the screening visit in every patient based on American College of Rheumatology (ACR) criteria or, if both knees met the criteria, based on the most affected knee as indicated by the patient. In case both knees were affected equally, the right knee was selected as the index knee. Demographic and clinical data, blood and urine samples, and imaging data were collected. Regarding imaging, QCT, MRI and X-ray examinations performed at study inclusion were used for the present cross-sectional analyses.

2.2. QCT acquisition and evaluation

QCT data were acquired from the index knee using six different scanners (A Coruña: GE Lightspeed VCT; Leiden: Toshiba Aquilion One; Oslo: Philips Brilliance 64, which during the study was replaced by a Toshiba Aquilion Prime; Paris: Siemens Somatom Definiton Edge; Utrecht: Philips IQon Spectral CT 64). All study centers used a tube voltage of 120 kV an exposure of 220 mAs and a reconstruction field of view of 330 mm. With a scan length of 15 cm this resulted in an effective dose of approximately 0.1 mSv ($CTDI_{vol} = 11$ mGy, DLP = 230 mGy cm). A European Spine Phantom (ESP, QRM Möhrendorf, Germany) was used for cross calibration to ensure equivalence of CT protocols across scanners. Based on the ESP scans, settings for table height, reconstruction kernel, slice thickness and reconstruction increment were selected as shown in supplementary **Table S1**. An in-scan calibration phantom (QRM BDC phantom) was placed beneath the knee during image acquisition in order to convert CT values to BMD [7].

QCT scans were analyzed with a dedicated image analysis software MIAF-Knee (MIAF: Medical Image Analysis Framework, University of Erlangen) version 2.2.1R to assess BMD at the femur and tibia. The analysis procedure started with an automatic 3D-segmentation of the distal femur and proximal tibia which was divided into five steps: 1) segmentation of periosteal and endosteal bone surfaces using 3D volume growing with local adaptive thresholds and morphological operations, 2) segmentation of the growth plates, 3) segmentation of the joint space, and 4) definition of anatomic coordinate systems relative to which 5) analysis volumes of interest (VOIs) were positioned [7]. VOIs consisted of the cortical bone plate (Cort) and subchondral (Sub), mid-epiphyseal (Mid) and juxtaphyseal (Juxta, adjacent to the physis) VOIs and were

defined as described earlier [7]. The previously described analysis revealed excellent precision results for BMD, even in the analysis of small VOIs [7].

First, a regression plane through the anatomic coordinate systems was fitted to the voxels defining the growth plate. Then, starting from each voxel of the periosteal surface that is located adjacent to the joint space, rays are cast perpendicular to this regression plane. The ray length, determined by the intersection with this plane, is divided into three sections of equal length defining the subchondral epiphyseal, the mid-epiphyseal, and the juxtaphyseal VOIs [7]. Fig. 1 shows the different epiphyseal locations after the segmentation process, which is largely automated but allows the operator to interact and correct. Analyses times vary between 5 and 10 min depending on the degree of OA as more severe OA requires more user interactions.

BMD was evaluated separately for each compartment (medial, lateral) and for the assumed articular surfaces covered and not covered by the meniscus [7,25]. In order to differentiate the epiphysis into a VOI covered and a VOI not covered by the menisci, the periosteal surface was extended along the direction of the shaft axis [25]. The resulting surface was eroded (or peeled) by a morphological operation using a spherical structuring element with a default radius of 1 cm. Finally the original subchondral bone surface was restored in the peeled surface [25]. The same approach using 1 cm as default radius was described before [25] and is based on an evaluation of Erbagci et al., who reported a range of 8.9 to 9.7 mm of coverage in normal lateral and of 7.8 to 11.7 mm in normal medial menisci [26]. Fig. 2 shows the result of the evaluation into coverage and un-coverage in illustrative fashion.

2.3. MRI acquisition and evaluation

MRI of the index knee was acquired using 1.5 T scanners at two centers (A Coruña: Ingenia CX, Philips Medical Systems, Netherlands; Oslo: Aera, Siemens Healthcare, Germany) and using 3 T scanners at the other centers (Utrecht: Ingenia or Achieva, Philips Medical Systems, Netherlands; Leiden: Ingenia, Philips Medical Systems, Netherlands; Paris: Skyra, Siemens Healthcare, Germany). The MRI protocol included triplanar intermediate-weighted fat-suppressed sequences and a coronal T1-weighted sequence. Details of sequence parameters are provided in supplementary Table S2.

MRI evaluation was performed using the semi-quantitative MRI Osteoarthritis Knee Score (MOAKS) instrument assessing meniscal extrusion by a senior musculoskeletal radiologist (FWR) with 17 years' experience of semi-quantitative assessment of knee OA at the time of reading [27]. The reader was blinded to all clinical data. Meniscal extrusion was scored in the anterior and mid-joint locations from 0 to 3 by using sagittal and coronal images. Grading for meniscal extrusion was performed as follows: Grade 0: <2 mm; Grade 1: 2 to 2.9 mm, Grade 2: 3–4.9 mm; Grade 3: >5 mm [27].

2.4. Radiography

Radiographs were evaluated centrally by one blinded experienced observer (rheumatologist and postdoc researcher) according to the Kellgren and Lawrence (KL) scoring system: 0 = no signs of osteoarthritis, 1 = possible osteophytic lipping, no joint space narrowing (JSN), 2 = definite osteophytes, possible JSN, 3 = definite JSN, moderate osteophytes, possible sclerosis 4 = large osteophytes, marked JSN, severe sclerosis [17,28]. In addition, femorotibial angle formed by the intersection of anatomical axes of the femur and tibia was assessed in the frontal plane. A neutral knee alignment was defined with a femorotibial angle of -2° to 2°. A femorotibial angle $<-2^{\circ}$ was defined as varus alignment, $>2^{\circ}$ as valgus alignment [29,30].

2.5. Statistical analysis

Data were checked for normality with the Shapiro–Wilk test. If the data were normally distributed an analysis of variance (ANOVA) was used for the comparisons of BMD at the different anatomical locations (Cort, Sub, Mid, Juxta) within the femur and within the tibia applying Bonferroni post hoc tests. For the comparisons of corresponding medial and lateral anatomic locations and regions covered or not covered by meniscus a two-tailed paired *t*-test was used. Only KL0 patients were analyzed for these comparisons. For the comparisons of corresponding anatomic locations between patients with varus alignment and patients with normal knee alignment a two-tailed unpaired t-test was used.

An ANOVA with Bonferroni post hoc test was employed for analyzing the relation of KL score and meniscal extrusion with ipsi-compartmental BMD. A two-tailed unpaired t-test was used to compare the ipsi-compartmental BMD between patients with KL0/1 to KL2–4. Multiple regression analyses were performed for age, sex and BMI for each anatomic location (Cort, Sub, Mid, Juxta) at the medial and lateral femur, respectively at the medial and lateral tibia.

Results are presented as mean and standard deviation. *P*-values below 0.05 were considered to indicate statistically significant differences. All analyses were conducted using SPSS 28 (IBM Corporation, Armonk, NY).

3. Results

Complete datasets of 275 (213 women, 62 men) patients were available that had radiographic KL grading, CT evaluation and MRI MOAKS readings. Mean age was 66.5 ± 7.1 years, body mass index was

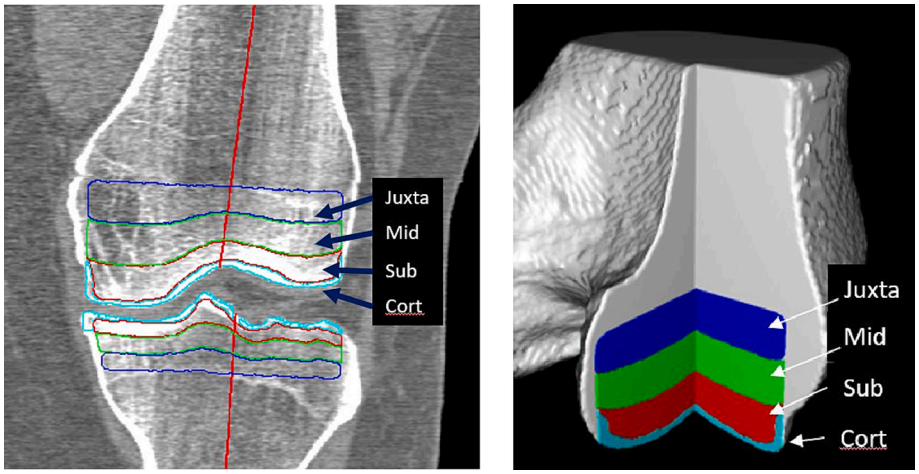

Fig. 1. Segmentation of the epiphyseal volume of interest (VOI) at the tibia and femur. A. Coronal CT reformat shows that three sections of equal length defining the subchondral epiphyseal (red), the mid-epiphyseal (green), and the juxtaphyseal (blue) epiphyseal locations were defined. In addition, the cortical bone plate (Cort) was segmented (light blue). The red line along the axis of the femur and the tibia divides the medial and lateral compartments of the femur and tibia. B. Three-dimensional rendering shows the segmentation result as a volume visualization [7]. (For interpretation of the references to colour in this figure legend, the reader is referred to the web version of this article.)

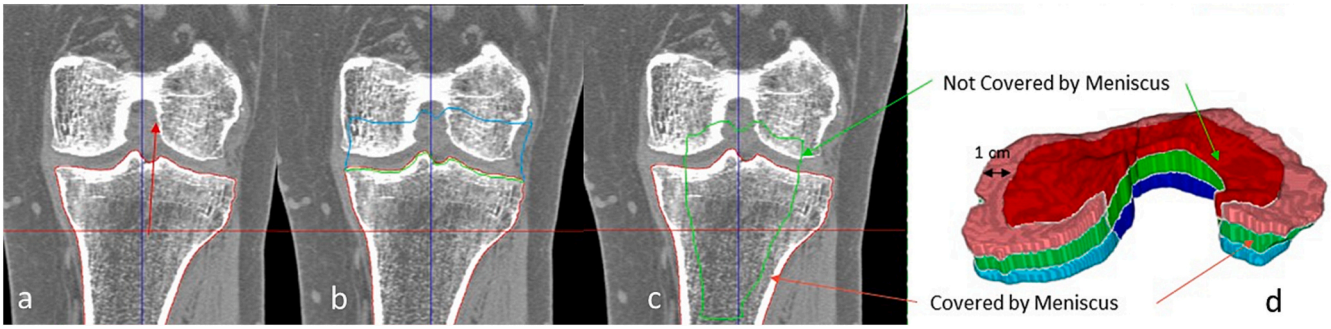

Fig. 2. Differentiation of the tibial surface into coverage and un-coverage by the meniscus. A volume of interest (VOI) assuming the meniscal coverage and a VOI of the tibial surface not covered by the menisci was defined by extending the periosteal surface along the direction of the shaft axis (a and b). The resulting surface was eroded (or peeled) by a morphological operation using a spherical structuring element with a default radius of 1 cm (c). Finally, the original subchondral bone surface was restored in the peeled surface. (d) exemplifies the resulting differentiation of the VOI not covered by the meniscus (dark red) and covered by the meniscus (light red). Adapted from [25]. (For interpretation of the references to colour in this figure legend, the reader is referred to the web version of this article.)

28.1 ± 5.3 kg/m^2. 52 knees were KL0, 71 KL1, 62 KL2, 79 KL3 and 11 knees were KL4. The mean femorotibial angle of our study cohort was −3.6° ± 2.8° (<−2° in 211 patients, −2° to 2° in 58 patients, >2° in 6 patients). Patients with varus malalignment exhibit a mean KL grade of 1.8 and patients with a normal knee alignment a KL grade of 1.5. Any (coronal and/or anterior) medial meniscal extrusion was present in 162 patients (grade 1: 68, grade 2: 58, grade 3: 36) and any lateral meniscal extrusion in 44 patients (grade 1: 15, grade 2: 16, grade 3: 13).

For KL0 knees, mean BMD differed significantly between each anatomic location (Cort, Sub, Mid, Juxta) with a decrease in BMD with increasing distance from the articular surface. In these participants without any signs of radiographic OA, these differences were statistically significant at both the femur and tibia (Table 1). Table 2 and Fig. 3 depict these findings for the medial and lateral femur and medial and lateral tibia.

Regarding the comparison between the medial and lateral compartment for KL0 knees, at the tibia, all anatomic locations showed higher BMD at the medial articular surface compared to the corresponding lateral one ($p < 0.001$). At the femur, higher BMD was observed for medial Cort and at the lateral Sub, Mid and Juxta locations compared to the corresponding other femoral compartment ($p < 0.001$) (Table 2).

In KL0 knees without meniscal extrusion, tibial regions (medial and lateral) assumed to be covered by the meniscus showed lower BMD at the Sub location ($p < 0.001$), showed equivalent BMD at the Mid ($p = 0.108$) and higher BMD at the Juxta location ($p < 0.001$) compared to regions not covered with meniscus (Table 3).

Knees with radiographic OA (KL2–4) presented with lower Sub ($p = 0.03$), Mid ($p = 0.01$) and Juxta ($p < 0.05$) BMD at the medial femur compared to KL0/1 knees (Table 4). At the medial tibia, comparisons of KL0/1 with KL2–4 revealed no significant differences. Cort BMD at the medial tibia was greater in KL4 compared to KL0 ($p < 0.001$). The results according to KL grades and comparing knees without and with radiographic OA are shown in Table 4. At the lateral femur, knees with KL2–4 showed lower BMD at Sub ($p \leq 0.01$), Mid ($p < 0.001$) and Juxta ($p = 0.01$) compared to KL0/1. The Cort BMD at the lateral tibia in KL2–4 was greater compared to KL0/1 (Table S3).

Across all KL grades, medial meniscal extrusion grade 2 and 3 was associated with greater BMD at the medial tibial Cort ($p < 0.001$, $p = 0.007$) compared to patients without extrusion. Only medial extrusion grade 3 showed greater BMD also at the medial femoral Cort ($p = 0.02$) compared to those without. Lateral meniscal extrusion grade 2 revealed greater BMD at the lateral tibial Cort ($p < 0.001$) compared to patients without extrusion. Lateral meniscal extrusion grade 3 was associated with greater BMD at the lateral Cort and Sub ($p < 0.001$, $p < 0.001$) of the tibia and at the lateral Cort ($p < 0.001$) of the femur compared to those without extrusion (Table 5).

Patients with varus malalignment exhibit significant greater BMD values at both the medial femur and the medial tibia at each anatomic locations (Cort, Sub, Mid, Juxta) compared to patients with normal knee alignment (Table 6). Table S4 for provides the evaluation of the lateral tibia and lateral femur in regard of the knee alignment.

Multiple regression analyses at each anatomic location (Cort, Sub, Mid, Juxta) at the medial femur and medial tibia revealed adjusted R^2 ranging from 0.10 to 0.18 for age, sex and BMI indicating weak to moderate goodness-of-fit. Significant negative regressions for BMD occurred for age and female gender at all anatomic locations at the medial femur and at the medial tibia. BMI showed significant positive regressions for BMD at all anatomic locations at the medial femur and at the medial tibia with exception for Cort (Table 7). Multiple regression analyses for the lateral femur and the later tibia are provided in Table S5.

Table 1
BMD at the cortical bone plate (Cort) and at the epiphysis at three different locations (subchondral epiphysis (Sub), mid-epiphysis (Mid) and juxtaphysis (Juxta)) at the femur and at the tibia for all participants with KL0. *P*-values are representative for the comparison of BMD between different anatomic locations within the femur or tibia. Significant *p*-values are emboldened.

BMD	Femur				Tibia			
	Mean [mg/cm^3]	SD		p-Value	Mean [mg/cm^3]	SD		p-Value
Cort	461.5	49.7	Cort vs Sub	**<0.001**	419.6	50.5	Cort vs Sub	**<0.001**
			Cort vs Mid	**<0.001**			Cort vs Mid	**<0.001**
			Cort vs Juxta	**<0.001**			Cort vs Juxta	**<0.001**
Sub	265.5	42.0	Sub vs Mid	**<0.001**	225.9	37.9	Sub vs Mid	**<0.001**
			Sub vs Juxta	**<0.001**			Sub vs Juxta	**<0.001**
Mid	199.2	37.1	Mid vs Juxta	**<0.001**	160.6	33.6	Mid vs Juxta	**<0.001**
Juxta	155.5	32.2			121.0	29.5		

Table 2
BMD at the cortical bone plate (Cort) and at the epiphysis at three different locations (subchondral epiphysis (Sub), mid-epiphysis (Mid) and juxtaphysis (Juxta)) at the medial and lateral femur and at the medial and lateral tibia for all participants with KL0. P-values are representative for the comparison of medial and lateral BMD within one anatomic location. Significant p-values are emboldened.

BMD	Femur					Tibia				
	Medial		Lateral			Medial		Lateral		
	Mean [mg/cm^3]	SD	Mean [mg/cm^3]	SD	p-Value	Mean [mg/cm^3]	SD	Mean [mg/cm^3]	SD	p-Value
Cort	498.0	58.1	429.0	47.5	**<0.001**	439.2	54.0	395.6	58.8	**<0.001**
Sub	262.1	45.6	270.1	41.6	**<0.001**	244.9	47.3	210.0	38.0	**<0.001**
Mid	178.3	37.9	223.3	39.3	**<0.001**	187.0	41.4	136.7	30.1	**<0.001**
Juxta	135.0	33.9	178.5	32.8	**<0.001**	140.4	34.9	103.8	27.2	**<0.001**

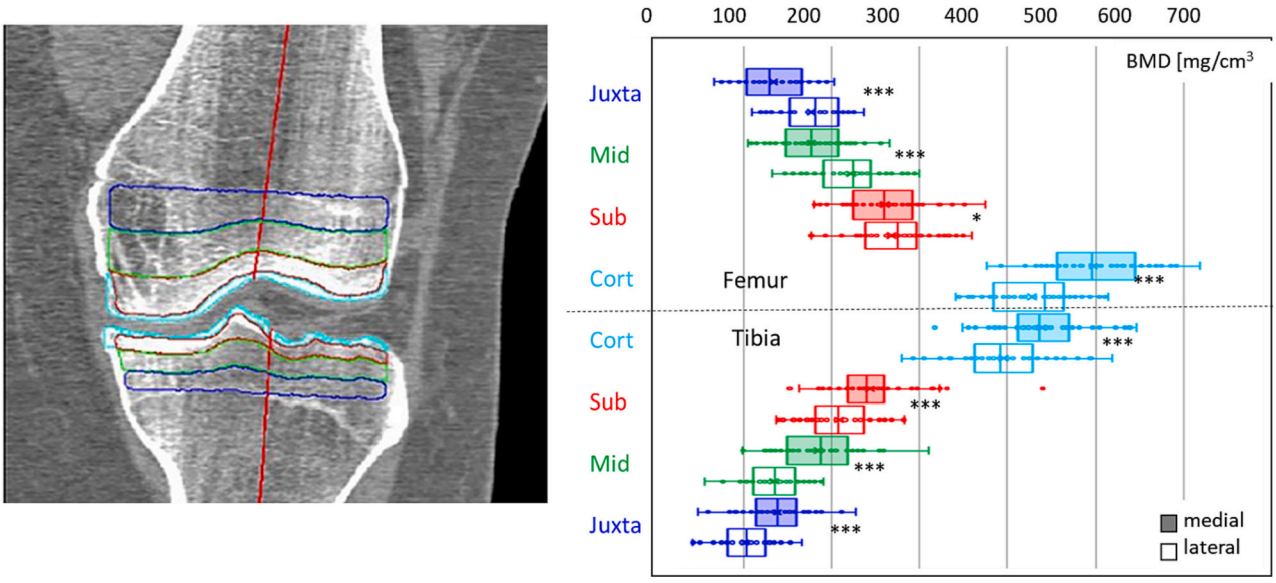

Fig. 3. Bone mineral density (BMD) for the different joint plates (medial and lateral femur, medial and lateral tibia) for all participants with KL0. BMD decreases with increasing distance from the articular surface in all joint plates. (Juxta = juxtaphysis location (dark blue), Mid = mid-epiphyseal location (green), Sub = subchondral epiphyseal location (red), Cort = cortical bone plate location (light blue)). BMD differs significantly between medial and lateral compartments (***: $p < 0.001$, *: $p < 0.1$). BMD also differed between Cort, Sub, Mid, and Juxta locations at both the femur and tibia. (For interpretation of the references to colour in this figure legend, the reader is referred to the web version of this article.)

Table 3
Impact of assumed meniscal coverage as shown in Fig. 2 on the tibial BMD. BMD at the tibial epiphysis at three different locations (subchondral epiphysis (Sub), mid-epiphysis (Mid) and juxtaphysis (Juxta)) of regions covered by meniscus and regions not covered by meniscus in participants with KL0 and no signs of meniscal extrusion. *P*-values are given for the comparison of corresponding anatomic locations covered and not covered by meniscus. Significant *p*-values are emboldened.

BMD	Tibia				
	Meniscal coverage		No meniscal coverage		
	Mean [mg/cm^3]	SD	Mean [mg/cm^3]	SD	p-value
Sub	187.6	33.3	234.9	45.2	**<0.001**
Mid	156.2	37.8	152.7	32.8	0.11
Juxta	130.2	34.6	102.9	27.8	**<0.001**

4. Discussion

Our evaluation of periarticular epiphyseal BMD in the IMI-APPROACH cohort revealed a significant decrease of BMD within the epiphyses of the tibia and femur with increasing distance from the joint in patients with KL0. This finding was consistent for the medial and lateral tibio-femoral joint compartment. In addition, in patients with KL 0 subchondral BMD at the tibia with assumed meniscal coverage was lower compared to locations not covered by meniscus, whereas the epiphysis adjacent to the physis was characterized by greater BMD in regions covered with meniscus. Finally, more severe structural OA showed greater cortical BMD values at the tibia and lower BMD at the femur at the subchondral level and beneath. Greater cortical and subchondral femoral and tibial BMD was observed in ipsi-lateral compartments with meniscal extrusion grade 2 and 3. Varus malalignment is associated with significant greater BMD values at both the medial femur and the medial tibia in all assessed anatomic locations (Cort, Sub, Mid, Juxta) compared to normal knee alignment.Bone is thought to play an important role in OA pathophysiology and QCT analysis has been used as a non-invasive imaging biomarker that provides information on bone changes at the knee [31]. Some in-vivo studies have used dual x-ray absorptiometry (DXA) to analyze BMD in OA, but the two-dimensional nature of DXA limits the assessment of spatial variations and localized alterations in BMD [12,32–35]. A few studies have also used CT for BMD assessment in knee OA, but, in contrast to the current study, most of them performed 2-D slice-based analyses or analyzed superficial regions of the epiphysis only [13,36,37].

While there is consensus that BMD is an important parameter that is affected by the course of the disease, it is still speculative how BMD varies locally in different stages of the disease [7,38]. As knee OA is considered to be a largely mechanically-driven disease, bone alterations likely play an important role in OA development, because bone adapts to loads by remodeling to meet its mechanical demands [39]. In our study we found a significant decrease of BMD within the epiphyses of the tibia

Table 4
BMD at the cortical bone plate (Cort) and at the epiphysis at three different locations (subchondral epiphysis (Sub), mid-epiphysis (Mid) and juxtaphysis (Juxta)) at the medial femur and at the medial tibia separated according to Kellgren-Lawrence grade (KL). REF = reference. ROA = radiological osteoarthritis. P-values are representative for the comparison of KL 0/1 with KL 2–4 and KL 0 to KL grades 1, 2, 3 or 4 for each anatomic location at the medial femur and at the medial tibia. Significant p-values are emboldened.

Medial	KL	Femur			Tibia		
		Mean [mg/cm^3]	SD	p-Value	Mean [mg/cm^3]	SD	p-Value
Cort	No ROA (KL 0/1)	486.78	61.03	REF	436.83	54.92	REF
	ROA (KL 2–4)	493.66	85.70	0.23	448.81	72.41	0.60
	0	498.01	58.11	REF	439.17	54.00	REF
	1	478.56	62.20	1.00	435.12	55.90	1.00
	2	474.66	77.80	0.96	424.99	57.39	1.00
	3	501.32	85.77	1.00	456.54	71.43	1.00
	4	545.71	104.53	0.55	527.57	92.07	<0.001
Sub	No ROA (KL 0/1)	255.98	49.14	REF	243.83	52.01	REF
	ROA (KL 2–4)	243.37	58.33	0.03	243.70	60.64	0.49
	0	262.05	45.64	REF	244.87	47.35	REF
	1	251.52	51.41	1.00	243.08	55.49	1.00
	2	240.86	58.68	0.40	241.67	67.04	1.00
	3	247.35	56.43	1.00	241.97	56.94	1.00
	4	228.96	71.69	0.68	267.57	46.22	1.00
Mid	No ROA (KL 0/1)	174.99	41.57	REF	183.53	44.99	REF
	ROA (KL 2–4)	162.04	47.98	0.01	176.55	52.72	0.12
	0	178.29	37.94	REF	186.95	41.42	REF
	1	172.57	44.15	1.00	181.02	47.56	1.00
	2	162.28	51.48	0.60	175.69	52.54	1.00
	3	165.35	44.19	1.00	174.31	51.77	1.00
	4	136.94	50.77	0.06	197.49	60.75	1.00
Juxta	No ROA (KL 0/1)	132.71	36.76	REF	136.35	38.44	REF
	ROA (KL 2–4)	124.42	43.99	<0.05	129.62	43.18	0.09
	0	134.99	33.89	REF	140.43	34.89	REF
	1	131.03	38.88	1.00	133.36	40.84	1.00
	2	124.75	48.88	1.00	127.48	41.29	0.96
	3	126.85	39.99	1.00	129.99	43.23	1.00
	4	105.06	41.38	0.28	139.01	55.28	1.00

Table 5
BMD at the cortical bone plate (Cort) and at the epiphysis at three different locations (subchondral epiphysis (Sub), mid-epiphysis (Mid) and juxtaphysis (Juxta)) at the femur and at tibia separated according to severity of maximal meniscal extrusion (grade 0–3). BMD is provided for ipsi-compartmental meniscal extrusion. REF = reference. P-values are representative for the comparison of patients without meniscal extrusion (grade 0) to patients with meniscal extrusion (grade 1–3) for each anatomic location at the femur and at the tibia.

Medial extrusion		Medial femur			Medial tibia		
	Grade	Mean [mg/cm^3]	SD	p-Value	Mean [mg/cm^3]	SD	p-Value
Cort	0	473.04	69.65	REF	425.17	60.11	REF
	1	496.64	64.11	0.21	443.22	53.63	0.36
	2	503.07	84.56	0.07	465.75	75.13	**<0.001**
	3	514.41	83.71	**0.02**	464.41	67.84	**0.01**
Sub	0	238.50	51.45	REF	233.23	53.69	REF
	1	258.67	55.46	0.08	253.34	69.06	0.12
	2	258.67	54.50	0.12	253.94	48.86	0.13
	3	248.73	56.78	1.00	247.13	49.63	1.00
Mid	0	162.23	43.69	REF	171.86	48.20	REF
	1	177.69	46.31	0.15	187.42	53.80	0.22
	2	169.93	46.83	1.00	185.84	47.64	0.45
	3	162.66	44.66	1.00	178.88	44.42	1.00
Juxta	0	123.41	40.05	REF	125.88	39.05	REF
	1	137.42	40.09	0.15	139.58	44.50	0.17
	2	128.90	43.52	1.00	136.11	42.52	0.71
	3	123.07	39.92	1.00	134.65	37.44	1.00

Lateral Extrusion		Lateral femur			Lateral tibia		
	Grade	Mean [mg/cm^3]	SD	p-Value	Mean [mg/cm^3]	SD	p-Value
Cort	0	421.31	57.95	REF	394.82	58.98	REF
	1	425.66	70.95	1.00	427.04	57.70	0.26
	2	455.65	59.00	0.15	474.79	71.95	**<0.001**
	3	495.61	66.67	**<0.001**	484.84	56.98	**<0.001**
Sub	0	252.85	49.37	REF	205.81	42.56	REF
	1	257.83	58.71	1.00	220.26	69.02	1.00
	2	250.33	49.80	1.00	234.92	71.80	0.10
	3	270.12	37.93	1.00	248.01	55.32	**0.01**
Mid	0	209.95	49.39	REF	128.97	37.54	REF
	1	212.87	52.92	1.00	130.27	41.75	1.00
	2	200.31	48.10	1.00	132.95	51.47	1.00
	3	208.12	44.03	1.00	150.67	33.10	0.29
Juxta	0	169.74	43.18	REF	96.60	33.57	REF
	1	173.97	45.96	1.00	100.37	40.83	1.00
	2	159.67	40.95	1.00	96.45	46.14	1.00
	3	165.04	40.76	1.00	100.21	33.68	1.00

and femur with increasing distance from the articular surface in symptomatic patients without signs of radiographic OA (KL0). These results are in line with the histomorphometric and μCT findings of Kamibayashi et al. [40] and μCT data from Touraine et al. [33], who showed decreasing bone volume fractions at the medial tibia in specimens with increasing distance of the articular surface. Lowitz et al. used the same approach that was used in the current study by applying QCT to 57 cadaver knees showing also a decrease of BMD with increasing distance to the joint [41]. However, in that study radiographic disease severity was not reported. [41].

The menisci at the knee play a relevant role in load bearing, shock absorption, and joint congruity and stability [42]. A micro-CT study showed that a degenerative medial meniscus in knee cadavers from OA subjects still retained some protective effect against osteoarthritis-induced subchondral bone changes [43]. Another study assessed cadaver knees with little or no signs of osteoarthritis using micro-CT and found higher values for bone volume fraction in regions of the subchondral bone that were not covered by meniscus [44]. Based on our investigation evaluating patients with KL0 we can confirm these findings for the subchondral bone in-vivo. Interestingly, the relationship of BMD between uncovered and covered regions by the meniscus is reversed within deeper anatomic locations adjacent to the metaphysis (Juxta) showing higher BMD for regions covered by meniscus, which was also reported in an earlier in-vivo study in patients with established radiographic OA [25]. These vertical differences of BMD within in the epiphysis may reflect differences in local loading related in part to the presence or absence of meniscal coverage [44]. Another possible explanation for the greater BMD near the periosteum relative to the density in the middle of the tibia in the juxtaphyseal epiphysis might be that this is simply a natural transition to a structurally optimal

Table 6
BMD at the cortical bone plate (Cort) and at the epiphysis at three different locations (subchondral epiphysis (Sub), mid-epiphysis (Mid) and juxtaphysis (Juxta)) at the medial femur and at the medial tibia for participants with varus alignment and with normal knee alignment. *P*-values are representative for the comparison of BMD between different anatomic locations within the medial femur or medial tibia. Significant *p*-values are emboldened.

BMD	Medial Femur					Medial Tibia				
	Varus		Normal alignement			Varus		Normal alignement		
	Mean [mg/cm^3]	SD	Mean [mg/cm^3]	SD	p-Value	Mean [mg/cm^3]	SD	Mean [mg/cm^3]	SD	p-Value
Cort	505.4	70.5	458.8	73.8	**<0.001**	451.9	63.2	423.7	62.5	**0.001**
Sub	260.8	49.6	223.1	55.9	**<0.001**	254.9	56.4	220.3	49.8	**<0.001**
Mid	176.0	41.5	148.4	49.0	**<0.001**	189.9	46.3	157.4	48.3	**<0.001**
Juxta	134.1	37.4	113.4	46.3	**0.001**	141.0	38.3	114.5	42.0	**<0.001**

Table 7
Multiple regression analyses at each anatomic location (Cort, Sub, Mid, Juxta) at the medial femur and medial tibia for age, sex and BMI. Negative regression coefficients for sex imply a decrease of BMI for women. Significant *p*-values are emboldened.

Regression	Medial Femur				Medial Tibia			
	Adjusted R^2		Regression coefficient	p-Value	Adjusted R^2		Regression Coefficient	p-Value
Cort	0.10	Age	−1.9	**0.003**	0.18	Age	−1.9	**<0.001**
		Sex	−46.4	**<0.001**		Sex	−55.3	**<0.001**
		BMI	1.3	0.12		BMI	1.0	0.18
Sub	0.13	Age	−1.1	**0.012**	0.11	Age	−1.2	**0.013**
		Sex	−31.0	**<0.001**		Sex	−22.7	**0.004**
		BMI	2.3	**<0.001**		BMI	2.6	**<0.001**
Mid	0.13	Age	−1.0	**0.007**	0.11	Age	−1.3	**0.001**
		Sex	−25.8	**<0.001**		Sex	−20.9	**0.002**
		BMI	2.0	**<0.001**		BMI	1.7	**0.002**
Juxta	0.14	Age	−0.8	**0.02**	0.17	Age	−1.2	**<0.001**
		Sex	−20.5	**<0.001**		Sex	−26.2	**<0.001**
		BMI	2.0	**<0.001**		BMI	1.7	**<0.001**

configuration of the bone without any relation to meniscal coverage [45].

It is well known from radiographs that subchondral bone sclerosis occurs in parallel with progression of OA [31]. Subchondral bone sclerosis is the result of new bone deposits on existing trabeculae, compression of the trabeculae, and callus formation on the fractured trabeculae and is one of the parameters used to define structural disease severity [31,46]. We also observed a tendency of greater BMD with increasing KL grades at the cortical bone plate of the femur and tibia in our study cohort revealing significant changes at the medial and lateral tibia. This is in line with a study using weight bearing knee CT of 33 patients applying cortical bone mapping. Greater tibial and femoral subarticular bone thickness and attenuation measurements in the medial joint space with worsening KL grade was reported, which could be taken as a quantitative correlate of subchondral sclerosis [47].

However, perhaps more interesting in terms of preventing the occurrence of osteoarthritis or slowing its progression is the observation of a reduced BMD in all other anatomic locations of the epiphysis (Sub, Mid and Juxta) of the medial and lateral femur with increasing OA disease severity [48]. Subchondral bone with reduced BMD may be less able to absorb and dissipate energy, thereby increasing forces transmitted through the joint and predisposing the articular surface to deformation and affect the overlying cartilage [39]. Our findings are in line with Patel et al., who used micro-CT in a small sample of cadaver knees assessing cores of the superficial 6 mm of the epiphysis [49]. They reported decreased bone volume fraction in cadavers with OA compared to normal knees [49]. In contrast to the femur no changes of BMD at Sub, Mid and Juxta levels occurred at the medial and lateral tibia with increasing OA severity in our study. However, the first 6 mm below the subchondral plate are distinctly different from the trabecular bone structure further below, thus the study from Patel may not be representative for the entire epiphyseal volume [43,44].

Besides alterations of the subchondral bone, patients with pathologies of the meniscus including extrusion or patients after meniscectomy are at increased risk of developing osteoarthritis or accelerated progression [50,51]. In animal studies and in humans an increased bone volume fraction was found after meniscectomy [52,53]. In our sample greater cortical and subchondral BMD at the femur and at the tibia were observed in ipsi-lateral compartments with meniscal extrusion grade 2 and 3, which suggest adaptation to changes in the mechanical environment of the knee [54]. However, these potential changes in mechanical load do not seem to have any impact on the mid-epiphysis (Mid) and parts of the epiphysis adjacent to the metaphysis (Juxta) at both the femur and the tibia.

An increased use of CT in OA research may be expected in the future. CT allows visualization of relevant OA-related tissue disease without the shortcoming of superimposition inherent to radiography. In addition, the introduction of weight-bearing (WB) cone-beam extremity CT allows imaging under physiologic loading conditions. Thus, WB-CT can be used to obtain tibio-femoral joint space width measurements at the knee joint without the projectional issues encountered with the application of radiography [55]. While data on BMD measures or bone structure from WB-CT systems is not available today, likely these systems will allow quantification of bone parameters under physiologic weight-bearing conditions including a more realistic assessment of meniscal position.

In comparison to previously published data assessing bone density at the knee regardless of the used approach and the severity of OA, the IMI-APPROACH cohort reflects a relatively large and well-defined sample. However, our results are limited by an unequal distribution of participants between subgroups of different grades of OA and by a limited number of patients with meniscal extrusion. In addition, our analysis based on KL grades does not enable any differentiation of medial or lateral OA. Thus, results in Tables 3 and S3 are dominated by the higher prevalence of medial OA. It must be considered that BMD assessed with QCT is an apparent density, as the volume of interest in which BMD is measured does not only consists of pure bone mineral but also contains non-mineralized Haversian canals, blood vessels, resorption cavities, bone marrow, and fat [31]. Hence, the evaluated BMD in the present study has to be distinguished from true tissue mineral density defined as the weight of ash per unit volume of bone free of empty spaces or non-

mineralized tissues, which is not feasible to perform in an in-vivo study [31]. Additional limitations of our study include the cross-sectional nature of our analysis, the focus on BMD only and the missing comparability to other measures of subchondral bone, e.g. bone structure as assessed by fractal signature analysis or other methods [56]. In addition, we did not assess the impact of different types of meniscal tears or substance loss. A further limitation is the assumption of a meniscal coverage of 1 cm as default radius, because coverage is not only patient specific but also varies between lateral and medial compartments. However, an average of 1 cm seems to be a reasonable assumption as accurate assessments of meniscal coverage from CT images cannot be obtained.

Targeting the pathways that modify subchondral bone turnover is an attractive option for disease modifying-OA drug (DMOAD) development as both, alterations in both composition and structural organization, lead to adverse effects on the overlying articular cartilage [16]. Clinical phenotypes, and molecular and imaging biomarkers characterizing these are currently being identified, but the exact interplay among them and underlying mechanisms of each remain to be elucidated [57]. While these biomarkers may have potential benefits in detecting those patients with the greatest risk for structural progression, their use still needs to be translated into more efficient clinical trial design and eventually clinical application [58]. Subchondral BMD may be one of the biomarkers characterizing a structural bone phenotype further in the future.In summary, in patients with clinical symptoms of OA and structurally normal knees vertical differences with decreasing BMD at both the medial and lateral femur and tibia are seen with increasing distance to the joint. Meniscal coverage seems to have a protective effect on subchondral bone, as it is associated with lower subchondral BMD suggesting shock absorption in weight-bearing regions of the knee joint. More severe structural OA shows greater cortical BMD values at the medial tibia and lower BMD at the medial femur at the subchondral level and levels beneath, whereas meniscal extrusion is associated with greater ipsi-lateral cortical and subchondral BMD at both the femur and tibia.

Ethical approval

All procedures performed in the IMI-Approach study were conducted in compliance with the protocol, Good Clinical Practice (GCP), the Declaration of Helsinki, and the applicable ethical and legal regulatory requirements (for all countries involved), and is registered under clinicaltrials.gov identifier: NCT03883568. Informed consent was obtained from all individual participants included in the study.

CRediT authorship contribution statement

Rafael Heiss: Conceptualization, Methodology, Validation, Formal analysis, Writing – original draft, Visualization. **Jean-Denis Laredo:** Conceptualization, Investigation, Writing – review & editing, Supervision, Project administration. **Wolfgang Wirth:** Conceptualization, Formal analysis, Data curation, Writing – review & editing, Project administration. **Mylène P. Jansen:** Conceptualization, Investigation, Data curation, Writing – review & editing, Supervision, Project administration. **Anne C.A. Marijnissen:** Conceptualization, Investigation, Writing – review & editing, Supervision, Project administration. **Floris Lafeber:** Conceptualization, Investigation, Writing – review & editing, Supervision, Project administration. **Agnes Lalande:** Conceptualization, Investigation, Writing – review & editing, Supervision, Project administration. **Harrie H. Weinans:** Conceptualization, Investigation, Writing – review & editing, Supervision, Project administration. **Francisco J. Blanco:** Conceptualization, Investigation, Writing – review & editing, Supervision, Project administration. **Francis Berenbaum:** Conceptualization, Investigation, Writing – review & editing, Supervision, Project administration. **Margreet Kloppenburg:** Conceptualization, Investigation, Writing – review & editing, Supervision, Project administration. **Ida K. Haugen:** Conceptualization, Investigation, Writing – review & editing, Supervision, Project administration. **Klaus Engelke:** Conceptualization, Methodology, Software, Validation, Formal analysis, Data curation, Writing – original draft, Writing – review & editing, Visualization, Project administration. **Frank W. Roemer:** Conceptualization, Methodology, Validation, Data curation, Writing – original draft, Writing – review & editing, Visualization, Project administration, Funding acquisition.

Declaration of competing interest

FWR is shareholder of Boston Imaging Core Lab. (BICL), LLC. He is consultant to Calibr and Grünenthal; RH is a member of the speakers bureau and a consultant of Siemens Healthineers, outside the submitted work. MK reports grants from IMI-APPROACH, during the conduct of the study; consulting fees from GlaxoSmithKline, Pfizer, Merck-Serono, Kiniksa, Abbvie, Flexion, Galapagos, Jansen, CHDR, UCB, Novartis outside the submitted work and all paid to institution; FJB funding from Gedeon Richter Plc., Bristol-Myers Squibb International Corporation (BMSIC), Sun Pharma Global FZE, Celgene Corporation, Janssen Cilag International N·V, Janssen Research & Development, Viela Bio, Inc., Astrazeneca AB, UCB BIOSCIENCES GMBH, UCB BIOPHARMA SPRL, AbbVie Deutschland GmbH & Co.KG, Merck KGaA, Amgen, Inc., Novartis Farmacéutica, S.A., Boehringer Ingelheim España, S.A, CSL Behring, LLC, Glaxosmithkline Research & Development Limited, Pfizer Inc., Lilly S.A., Corbus Pharmaceuticals Inc., Biohope Scientific Solutions for Human Health S.L., Centrexion Therapeutics Corp., Sanofi, MEIJI FARMA S.A., Kiniksa Pharmaceuticals, Ltd. Grunenthal, Asofarma Mexico, Gebro Pharma, Roche, Galapagos, Regeneron; FB is shareholder of 4Moving Biotech and 4P,Pharma, reports personal fees from Boehringer, Bone Therapeutics, Expanscience, Galapagos, Gilead, GSK, Merck Sereno, MSD, Novartis, Pfizer, Roche, Sanofi, Servier, Peptinov, TRB Chemedica, Viatris. WW is employee and shareholder of Chondrometrics GmbH. AL is employee of Servier. The other authors declare no competing interests.

Data availability

Data will be made available on request.

Acknowledgments

This work was supported by the Innovative Medicines Initiative Joint Undertaking under grant agreement no 115770, resources of which are composed of financial contribution from the European Union's Seventh Framework Programme (FP7/2007-2013) and EFPIA companies' in kind contribution. See www.imi.europa.eu and www.approachproject.eu.

Appendix A. Supplementary data

Supplementary data to this article can be found online at https://doi.org/10.1016/j.bone.2023.116673.

References

[1] G.B.D. Disease, I. Injury, C. Prevalence, Global, regional, and national incidence, prevalence, and years lived with disability for 310 diseases and injuries, 1990–2015: a systematic analysis for the global burden of disease study 2015, Lancet 388 (10053) (2016) 1545–1602, https://doi.org/10.1016/S0140-6736(16)31678-6.

[2] D.J. Hunter, D. Schofield, E. Callander, The individual and socioeconomic impact of osteoarthritis, Nat. Rev. Rheumatol. 10 (7) (2014) 437–441, https://doi.org/10.1038/nrrheum.2014.44.

[3] E. Losina, A.M. Weinstein, W.M. Reichmann, S.A. Burbine, D.H. Solomon, M. E. Daigle, B.N. Rome, S.P. Chen, D.J. Hunter, L.G. Suter, J.M. Jordan, J.N. Katz, Lifetime risk and age at diagnosis of symptomatic knee osteoarthritis in the US, Arthritis Care Res. (Hoboken) 65 (5) (2013) 703–711, https://doi.org/10.1002/acr.21898.

[4] J.A. Buckwalter, H.J. Mankin, Articular cartilage: degeneration and osteoarthritis, repair, regeneration, and transplantation, Instr. Course Lect. 47 (1998) 487–504.
[5] G.H. Lo, E. Schneider, J.B. Driban, L.L. Price, D.J. Hunter, C.B. Eaton, M. C. Hochberg, R.D. Jackson, C.K. Kwoh, M.C. Nevitt, J.A. Lynch, T.E. McAlindon, O. A.I.I. Group, Periarticular bone predicts knee osteoarthritis progression: data from the osteoarthritis initiative, Semin Arthritis Rheum 48 (2) (2018) 155–161, https://doi.org/10.1016/j.semarthrit.2018.01.008.
[6] F. Intema, H.A. Hazewinkel, D. Gouwens, J.W. Bijlsma, H. Weinans, F.P. Lafeber, S. C. Mastbergen, In early OA, thinning of the subchondral plate is directly related to cartilage damage: results from a canine ACLT-meniscectomy model, Osteoarthr. Cartil. 18 (5) (2010) 691–698, https://doi.org/10.1016/j.joca.2010.01.004.
[7] P. Zerfass, T. Lowitz, O. Museyko, V. Bousson, L. Laouisset, W.A. Kalender, J. D. Laredo, K. Engelke, An integrated segmentation and analysis approach for QCT of the knee to determine subchondral bone mineral density and texture, IEEE Trans. Biomed. Eng. 59 (9) (2012) 2449–2458, https://doi.org/10.1109/TBME.2012.2202660.
[8] J.C. Baker-LePain, N.E. Lane, Role of bone architecture and anatomy in osteoarthritis, Bone 51 (2) (2012) 197–203, https://doi.org/10.1016/j.bone.2012.01.008.
[9] S.K. Boyd, R. Muller, J.R. Matyas, G.R. Wohl, R.F. Zernicke, Early morphometric and anisotropic change in periarticular cancellous bone in a model of experimental knee osteoarthritis quantified using microcomputed tomography, Clin. Biomech. (Bristol, Avon) 15 (8) (2000) 624–631, https://doi.org/10.1016/s0268-0033(00)00023-1.
[10] V.B. Kraus, S. Feng, S. Wang, S. White, M. Ainslie, A. Brett, A. Holmes, H. C. Charles, Trabecular morphometry by fractal signature analysis is a novel marker of osteoarthritis progression, Arthritis Rheum. 60 (12) (2009) 3711–3722, https://doi.org/10.1002/art.25012.
[11] W.D. Burnett, S.A. Kontulainen, C.E. McLennan, D. Hazel, C. Talmo, D.R. Wilson, D.J. Hunter, J.D. Johnston, Knee osteoarthritis patients with more subchondral cysts have altered tibial subchondral bone mineral density, BMC Musculoskelet. Disord. 20 (1) (2019) 14, https://doi.org/10.1186/s12891-018-2388-9.
[12] H. Babel, P. Omoumi, K. Cosendey, H. Cadas, B.M. Jolles, J. Favre, Three-dimensional quantification of bone mineral density in the distal femur and proximal tibia based on computed tomography: in vitro evaluation of an extended standardization method, J. Clin. Med. 10 (1) (2021), https://doi.org/10.3390/jcm10010160.
[13] J.D. Johnston, B.A. Masri, D.R. Wilson, Computed tomography topographic mapping of subchondral density (CT-TOMASD) in osteoarthritic and normal knees: methodological development and preliminary findings, Osteoarthr. Cartil. 17 (10) (2009) 1319–1326, https://doi.org/10.1016/j.joca.2009.04.013.
[14] P. Omoumi, H. Babel, B.M. Jolles, J. Favre, Quantitative regional and sub-regional analysis of femoral and tibial subchondral bone mineral density (sBMD) using computed tomography (CT): comparison of non-osteoarthritic (OA) and severe OA knees, Osteoarthr. Cartil. 25 (11) (2017) 1850–1857, https://doi.org/10.1016/j.joca.2017.07.014.
[15] W.D. Burnett, S.A. Kontulainen, C.E. McLennan, D.J. Hunter, D.R. Wilson, J. D. Johnston, Regional depth-specific subchondral bone density measures in osteoarthritic and normal patellae: in vivo precision and preliminary comparisons, Osteoporos. Int. 25 (3) (2014) 1107–1114, https://doi.org/10.1007/s00198-013-2568-2.
[16] M.A. Karsdal, M. Michaelis, C. Ladel, A.S. Siebuhr, A.R. Bihlet, J.R. Andersen, H. Guehring, C. Christiansen, A.C. Bay-Jensen, V.B. Kraus, Disease-modifying treatments for osteoarthritis (DMOADs) of the knee and hip: lessons learned from failures and opportunities for the future, Osteoarthr. Cartil. 24 (12) (2016) 2013–2021, https://doi.org/10.1016/j.joca.2016.07.017.
[17] E.M. van Helvoort, W.E. van Spil, M.P. Jansen, P.M.J. Welsing, M. Kloppenburg, M. Loef, F.J. Blanco, I.K. Haugen, F. Berenbaum, J. Bacardit, C.H. Ladel, J. Loughlin, A.C. Bay-Jensen, A. Mobasheri, J. Larkin, J. Boere, H.H. Weinans, A. Lalande, A.C.A. Marijnissen, F. Lafeber, Cohort profile: the applied public-private research enabling OsteoArthritis clinical headway (IMI-APPROACH) study: a 2-year, European, cohort study to describe, validate and predict phenotypes of osteoarthritis using clinical, imaging and biochemical markers, BMJ Open 10 (7) (2020), e035101, https://doi.org/10.1136/bmjopen-2019-035101.
[18] E.M. van Helvoort, C. Ladel, S. Mastbergen, M. Kloppenburg, F.J. Blanco, I. K. Haugen, F. Berenbaum, J. Bacardit, P. Widera, P.M.J. Welsing, F. Lafeber, Baseline clinical characteristics of predicted structural and pain progressors in the IMI-APPROACH knee OA cohort, RMD Open 7 (3) (2021), https://doi.org/10.1136/rmdopen-2021-001759.
[19] J. Wesseling, M. Boers, M.A. Viergever, W.K. Hilberdink, F.P. Lafeber, J. Dekker, J. W. Bijlsma, Cohort profile: cohort hip and cohort knee (CHECK) study, Int. J. Epidemiol. 45 (1) (2016) 36–44, https://doi.org/10.1093/ije/dyu177.
[20] W. Damman, R. Liu, F.P.B. Kroon, M. Reijnierse, T.W.J. Huizinga, F.R. Rosendaal, M. Kloppenburg, Do comorbidities play a role in hand osteoarthritis disease burden? Data from the hand osteoarthritis in secondary care cohort, J. Rheumatol. 44 (11) (2017) 1659–1666, https://doi.org/10.3899/jrheum.170208.
[21] K. Magnusson, K.B. Hagen, N. Osteras, L. Nordsletten, B. Natvig, I.K. Haugen, Diabetes is associated with increased hand pain in erosive hand osteoarthritis: data from a population-based study, Arthritis Care Res. (Hoboken) 67 (2) (2015) 187–195, https://doi.org/10.1002/acr.22460.
[22] N. Oreiro-Villar, A.C. Raga, I. Rego-Perez, S. Pertega, M. Silva-Diaz, M. Freire, C. Fernandez-Lopez, F.J. Blanco, PROCOAC (PROspective COhort of a Coruna) description: Spanish prospective cohort to study osteoarthritis, Reumatol. Clin. (Engl. Ed.) (2020), https://doi.org/10.1016/j.reuma.2020.08.010.
[23] J. Sellam, E. Maheu, M.D. Crema, A. Touati, A. Courties, S. Tuffet, A. Rousseau, X. Chevalier, B. Combe, M. Dougados, B. Fautrel, M. Kloppenburg, J.D. Laredo, D. Loeuille, A. Miquel, F. Rannou, P. Richette, T. Simon, F. Berenbaum, The DIGICOD cohort: a hospital-based observational prospective cohort of patients with hand osteoarthritis - methodology and baseline characteristics of the population, Joint Bone Spine 88 (4) (2021), 105171, https://doi.org/10.1016/j.jbspin.2021.105171.
[24] P. Widera, P.M.J. Welsing, C. Ladel, J. Loughlin, F. Lafeber, F. Petit Dop, J. Larkin, H. Weinans, A. Mobasheri, J. Bacardit, Multi-classifier prediction of knee osteoarthritis progression from incomplete imbalanced longitudinal data, Sci. Rep. 10 (1) (2020) 8427, https://doi.org/10.1038/s41598-020-64643-8.
[25] F. Sannmann, J.D. Laredo, C. Chappard, K. Engelke, Impact of meniscal coverage on subchondral bone mineral density of the proximal tibia in female subjects - a cross-sectional in vivo study using QCT, Bone 134 (2020), 115292, https://doi.org/10.1016/j.bone.2020.115292.
[26] H. Erbagci, E. Gumusburun, M. Bayram, G. Karakurum, A. Sirikci, The normal menisci: in vivo MRI measurements, Surg. Radiol. Anat. 26 (1) (2004) 28–32, https://doi.org/10.1007/s00276-003-0182-2.
[27] D.J. Hunter, A. Guermazi, G.H. Lo, A.J. Grainger, P.G. Conaghan, R.M. Boudreau, F.W. Roemer, Evolution of semi-quantitative whole joint assessment of knee OA: MOAKS (MRI osteoarthritis knee Score), Osteoarthr. Cartil. 19 (8) (2011) 990–1002, https://doi.org/10.1016/j.joca.2011.05.004.
[28] J.H. Kellgren, J.S. Lawrence, Radiological assessment of osteo-arthrosis, Ann. Rheum. Dis. 16 (4) (1957) 494–502, https://doi.org/10.1136/ard.16.4.494.
[29] D.T. Felson, J. Niu, T. Yang, J. Torner, C.E. Lewis, P. Aliabadi, B. Sack, L. Sharma, A. Guermazi, J. Goggins, M.C. Nevitt, Most, O.A.I. Investigators, Physical activity, alignment and knee osteoarthritis: data from MOST and the OAI, Osteoarthr. Cartilage 21 (6) (2013) 789–795, https://doi.org/10.1016/j.joca.2013.03.001.
[30] G. Micicoi, R. Khakha, K. Kley, A. Wilson, S. Cerciello, M. Ollivier, Managing intra-articular deformity in high tibial osteotomy: a narrative review, J. Exp. Orthop. 7 (1) (2020) 65, https://doi.org/10.1186/s40634-020-00283-1.
[31] V. Bousson, T. Lowitz, L. Laouisset, K. Engelke, J.D. Laredo, CT imaging for the investigation of subchondral bone in knee osteoarthritis, Osteoporos. Int. 23 (Suppl 8) (2012) S861–S865, https://doi.org/10.1007/s00198-012-2169-5.
[32] A. Sepriano, J.A. Roman-Blas, R.D. Little, F. Pimentel-Santos, J.M. Arribas, R. Largo, J.C. Branco, G. Herrero-Beaumont, DXA in the assessment of subchondral bone mineral density in knee osteoarthritis-a semi-standardized protocol after systematic review, Semin. Arthritis Rheum. 45 (3) (2015) 275–283, https://doi.org/10.1016/j.semarthrit.2015.06.012.
[33] O. Bruyere, C. Dardenne, E. Lejeune, B. Zegels, A. Pahaut, F. Richy, L. Seidel, O. Ethgen, Y. Henrotin, J.Y. Reginster, Subchondral tibial bone mineral density predicts future joint space narrowing at the medial femoro-tibial compartment in patients with knee osteoarthritis, Bone 32 (5) (2003) 541–545, https://doi.org/10.1016/S8756-3282(03)00059-0.
[34] S. Clarke, C. Wakeley, J. Duddy, M. Sharif, I. Watt, K. Ellingham, C.J. Elson, G. Nickols, J.R. Kirwan, Dual-energy X-ray absorptiometry applied to the assessment of tibial subchondral bone mineral density in osteoarthritis of the knee, Skelet. Radiol. 33 (10) (2004) 588–595, https://doi.org/10.1007/s00256-004-0790-x.
[35] A. Boudenot, S. Pallu, H. Toumi, S.L. Peres, E. Dolleans, E. Lespessailles, Tibial subchondral bone mineral density: sources of variability and reproducibility, Osteoarthr. Cartilage 21 (10) (2013) 1586–1594, https://doi.org/10.1016/j.joca.2013.07.009.
[36] A. Odgaard, C.M. Pedersen, S.M. Bentzen, J. Jorgensen, I. Hvid, Density changes at the proximal tibia after medial meniscectomy, J. Orthop. Res. 7 (5) (1989) 744–753, https://doi.org/10.1002/jor.1100070517.
[37] K.L. Bennell, M.W. Creaby, T.V. Wrigley, D.J. Hunter, Tibial subchondral trabecular volumetric bone density in medial knee joint osteoarthritis using peripheral quantitative computed tomography technology, Arthritis Rheum. 58 (9) (2008) 2776–2785, https://doi.org/10.1002/art.23795.
[38] S.R. Goldring, Role of bone in osteoarthritis pathogenesis, Med Clin North Am 93 (1) (2009) 25–35, https://doi.org/10.1016/j.mcna.2008.09.006, xv.
[39] T. Neogi, Clinical significance of bone changes in osteoarthritis, Ther. Adv. Musculoskelet. Dis. 4 (4) (2012) 259–267, https://doi.org/10.1177/1759720X12437354.
[40] L. Kamibayashi, U.P. Wyss, T.D. Cooke, B. Zee, Trabecular microstructure in the medial condyle of the proximal tibia of patients with knee osteoarthritis, Bone 17 (1) (1995) 27–35, https://doi.org/10.1016/8756-3282(95)00137-3.
[41] T. Lowitz, O. Museyko, V. Bousson, C. Chappard, L. Laouisset, J.D. Laredo, K. Engelke, Advanced knee structure analysis (AKSA): a comparison of bone mineral density and trabecular texture measurements using computed tomography and high-resolution peripheral quantitative computed tomography of human knee cadavers, Arthritis Res. Ther. 19 (1) (2017) 1, https://doi.org/10.1186/s13075-016-1210-z.
[42] A.J. Fox, F. Wanivenhaus, A.J. Burge, R.F. Warren, S.A. Rodeo, The human meniscus: a review of anatomy, function, injury, and advances in treatment, Clin. Anat. 28 (2) (2015) 269–287, https://doi.org/10.1002/ca.22456.
[43] G. Mitton, K. Engelke, S. Uk, J.D. Laredo, C. Chappard, A degenerative medial meniscus retains some protective effect against osteoarthritis-induced subchondral bone changes, Bone Rep 12 (2020), 100271, https://doi.org/10.1016/j.bonr.2020.100271.
[44] S. Touraine, H. Bouhadoun, K. Engelke, J.D. Laredo, C. Chappard, Influence of meniscus on cartilage and subchondral bone features of knees from older individuals: a cadaver study, PLoS One 12 (8) (2017), e0181956, https://doi.org/10.1371/journal.pone.0181956.
[45] K.J. Fischer, C.R. Jacobs, D.R. Carter, Computational method for determination of bone and joint loads using bone density distributions, J. Biomech. 28 (9) (1995) 1127–1135, https://doi.org/10.1016/0021-9290(94)00182-4.

[46] R.D. Altman, G.E. Gold, Atlas of individual radiographic features in osteoarthritis, revised, Osteoarthritis Cartilage 15 (Suppl A) (2007) A1–A56.
[47] T.D. Turmezei, S.B. Low, S. Rupret, G.M. Treece, A.H. Gee, J.W. MacKay, J. A. Lynch, K.E. Poole, N.A. Segal, Multiparametric 3-D analysis of bone and joint space width at the knee from weight bearing computed tomography, Osteoarthr. Imaging 2 (2) (2022), https://doi.org/10.1016/j.ostima.2022.100069.
[48] G.H. Lo, Y. Zhang, C. McLennan, J. Niu, D.P. Kiel, R.R. McLean, P. Aliabadi, D. T. Felson, D.J. Hunter, The ratio of medial to lateral tibial plateau bone mineral density and compartment-specific tibiofemoral osteoarthritis, Osteoarthr. Cartil. 14 (10) (2006) 984–990, https://doi.org/10.1016/j.joca.2006.04.010.
[49] V. Patel, A.S. Issever, A. Burghardt, A. Laib, M. Ries, S. Majumdar, MicroCT evaluation of normal and osteoarthritic bone structure in human knee specimens, J. Orthop. Res. 21 (1) (2003) 6–13, https://doi.org/10.1016/S0736-0266(02)00093-1.
[50] J.T. Badlani, C. Borrero, S. Golla, C.D. Harner, J.J. Irrgang, The effects of meniscus injury on the development of knee osteoarthritis: data from the osteoarthritis initiative, Am. J. Sports Med. 41 (6) (2013) 1238–1244, https://doi.org/10.1177/0363546513490276.
[51] H. Roos, M. Lauren, T. Adalberth, E.M. Roos, K. Jonsson, L.S. Lohmander, Knee osteoarthritis after meniscectomy: prevalence of radiographic changes after twenty-one years, compared with matched controls, Arthritis Rheum. 41 (4) (1998) 687–693, https://doi.org/10.1002/1529-0131(199804)41:4<687::AID-ART16>3.0.CO;2-2.
[52] A. Fahlgren, K. Messner, P. Aspenberg, Meniscectomy leads to an early increase in subchondral bone plate thickness in the rabbit knee, Acta Orthop. Scand. 74 (4) (2003) 437–441, https://doi.org/10.1080/00016470310017758.
[53] M.M. Petersen, C. Olsen, J.B. Lauritzen, B. Lund, A. Hede, Late changes in bone mineral density of the proximal tibia following total or partial medial meniscectomy. A randomized study, J. Orthop. Res. 14 (1) (1996) 16–21, https://doi.org/10.1002/jor.1100140105.
[54] A. Ariyachaipanich, E. Kaya, S. Statum, R. Biswas, B. Tran, W.C. Bae, C.B. Chung, MR imaging pattern of tibial subchondral bone structure: considerations of meniscal coverage and integrity, Skelet. Radiol. 49 (12) (2020) 2019–2027, https://doi.org/10.1007/s00256-020-03517-6.
[55] T.D. Turmezei, S. Rupret, G.M. Treece, A.H. Gee, J.W. MacKay, J.A. Lynch, K.E. S. Poole, N.A. Segal, BLS, Quantitative three-dimensional assessment of knee joint space width from weight-bearing CT, Radiology (2021) 203928, https://doi.org/10.1148/radiol.2021203928.
[56] V.B. Kraus, J.E. Collins, H.C. Charles, C.F. Pieper, L. Whitley, E. Losina, M. Nevitt, S. Hoffmann, F. Roemer, A. Guermazi, D.J. Hunter, O.A.B. Consortium, Predictive validity of radiographic trabecular bone texture in knee osteoarthritis: the Osteoarthritis Research Society International/Foundation for the National Institutes of Health Osteoarthritis Biomarkers Consortium, Arthritis Rheumatol 70 (1) (2018) 80–87, https://doi.org/10.1002/art.40348.
[57] A. Dell'Isola, R. Allan, S.L. Smith, S.S. Marreiros, M. Steultjens, Identification of clinical phenotypes in knee osteoarthritis: a systematic review of the literature, BMC Musculoskelet. Disord. 17 (1) (2016) 425, https://doi.org/10.1186/s12891-016-1286-2.
[58] W.M. Oo, C. Little, V. Duong, D.J. Hunter, The development of disease-modifying therapies for osteoarthritis (DMOADs): the evidence to date, Drug Des. Devel. Ther. 15 (2021) 2921–2945, https://doi.org/10.2147/DDDT.S295224.